

# Investigation on the origin of terahertz waves generated by dc-biased multimode semiconductor lasers at room temperature

Sylwester Latkowski, Frederic Surre, Ramon Maldonado-Basilio, and Pascal Landais<sup>a)</sup>  
*School of Electronic Engineering, Dublin City University, Glasnevin, Dublin 9, Ireland*

(Received 9 September 2008; accepted 26 November 2008; published online 18 December 2008)

A technique to measure a terahertz wave generated by spectrum tailored Fabry–Pérot lasers (FP) is assessed. A dc-biased and 25 °C temperature controlled FP is probed by a continuous wave signal, tuned at 20 nm away from its lasing modes. With a 0.02 nm resolution optical spectrum analyzer (OSA), the terahertz generated signal frequency is measured from the interval between the probe and its side-band modulations. The terahertz waves emitted by these FPs are measured at  $370 \pm 5$  GHz and at  $1.157 \pm 0.005$  THz, respectively, within a precision set by our OSA. The origin of the terahertz wave is due to passive mode-locked through intracavity four-wave-mixing processes. © 2008 American Institute of Physics. [DOI: 10.1063/1.3050455]

Recently we demonstrated the generation of a terahertz wave signal at 0.37 THz by a multimode semiconductor laser at room temperature.<sup>1</sup> This device is a Fabry–Pérot (FP) laser with a one-dimensional photonic band gap embedded in its structure. The photonic band gap is realized by etching shallow grooves on the *p* side of the laser junction perpendicular to the longitudinal axis of the device.<sup>2</sup> These grooves are not deep enough to reach the active layer but deep enough to affect the effective refractive index experienced by the electromagnetic wave generated in the active layer. By etching these grooves at key positions, it is possible to generate variation in the refractive index along the cavity and consequently to control the longitudinal spectrum.<sup>3</sup> In this device, the FP resonance fixed by the device length determines an initial spectral separation between consecutive modes but the etched band gap suppresses or enhances some specific FP modes. It is feasible therefore to engineer not only the number of lasing modes but also their free-spectral range (FSR). Thus, at least two optical signals can be selected. These modes beat together inside the laser cavity generating a signal at the intermediate frequency that in our case is within the terahertz regime. In our approach, the generated terahertz signal benefits from a good overlap between the spatial modes but also from the nonlinear effects in the semiconductor material, which is able to respond to a terahertz excitation. Compared to the photonic transmitter,<sup>4</sup> our solution does not require any external source, therefore it is more stable and its foot print is smaller. Moreover, with respect to a quantum cascade laser,<sup>5</sup> the dc-bias current applied is of the order of 100 mA for a voltage across the junction of <2 V, therefore its power consumption is small.

In this paper, we present an experimental investigation on the origin of the terahertz waves generated by multimode semiconductor lasers. In this investigation, it is assumed that the terahertz wave generated by our devices benefit from intracavity four-wave-mixing (FWM) processes and consequently that these lasers are passively mode-locked. First, this method was tested on a ~370 GHz wave generator multimode laser and it shows an excellent agreement with the results achieved by two other techniques of terahertz measurement.<sup>1</sup> Using the proposed method, we are able to

measure a 1.1 THz wave generated from a multimode semiconductor laser with a FSR of 1.1 THz, dc-biased and temperature controlled at 25 °C. Based on the conclusive output of this technique, we can argue that the most likely mechanism for terahertz wave generation in these devices is carrier heating (CH).

The first device under test (DUT) is a 350 μm long multi-quantum well InAlGaAs FP laser. Its 2 μm wide ridge waveguide provides a spatial single mode output. The grooves are 1 μm deep and 2 μm wide. The front facet has a reflection coefficient of 28% and the back one of 95%. The laser is characterized by a current threshold of  $I_{th} = 19$  mA at a constant temperature of 25 °C. In Fig. 1, the emission spectrum is presented for a bias current of 89.9 mA and a voltage of <2 V across the junction. It exhibits four modes, with a FSR of 3 nm resulting from the designed pattern of the shallow etched grooves on the *p* side. The observed 1 nm separation ripples are due to the FP resonance of the 350 μm cavity length. Under identical experimental conditions, two different methods were used to assess the performance of this device as a terahertz wave generator.<sup>1</sup> With the second harmonic generation frequency resolved optical gating (FROG) method, a modulation of the two main modes selected was observed at a frequency of ~370 GHz with a constant phase difference of  $\pi$  radians. These measurements were obtained by curve fitting to overcome the high noise level of the system. Second, with a 1.8 GHz resolution Four-

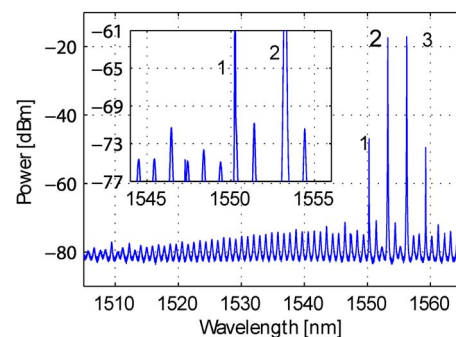


FIG. 1. (Color online) Optical spectrum of the first DUT biased at 89.9 mA and temperature controlled at 25 °C. The inset is a zoom of the spectrum around mode 1.

<sup>a)</sup>Electronic mail: landaisp@ceng.dcu.ie.

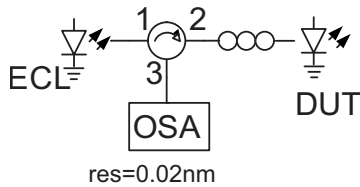


FIG. 2. Experimental setup of the method of investigation.

rier transform (FT) spectrometer, interfaced to a 3.6 K cooled bolometer, a clear signal at 0.7 THz corresponding to the second harmonic of the modulation measured by the FROG was detected. Both experimental techniques demonstrated the potential of this device as a terahertz wave generator but from these results it was not possible to further investigate the origin of the terahertz generation in this device. We attributed the narrow linewidth of the detected signal, below the resolution of the FT-IR spectrometer, to a FWM effect contributing to the phase synchronization of the lasing modes. This was illustrated by some FROG measurements, which presented a modulation of the second harmonic signal of the two main modes. The second harmonic traces were slightly penalized by amplitude noise due to the second harmonic generation. This experimental evidence was not demonstrated by any other measurement. However, with the experiment below, we can conclusively confirm this hypothesis.

In order to determine whether there is terahertz generation sustained by the gain nonlinearities, we propose the setup depicted in Fig. 2. The aim is to exploit the modulation supported by any FWM effects.<sup>6</sup> A continuous-wave signal from an external cavity laser is launched into our DUT via a circulator. The probe signal is at 1509.43 nm, with a 5.5 dBm power measured before port 1, while the lasing wavelengths of the DUT are centered at  $\sim 1555$  nm. With this detuning and power injected, the longitudinal spectrum of the laser is not modified, the perturbation due to FWM generated by the probe signal is minimized, and the detuning between the probe and laser modes is not comparable to the frequency to be measured. A polarization controller is placed before the DUT input to align the polarization of the probe field to the TE mode of the laser waveguide. The DUT is dc-biased at 89.9 mA and temperature controlled at 25 °C. The output signal of the DUT is collected from port 3 and observed on a 0.02 nm resolution optical spectrum analyzer (OSA).

The output spectrum is depicted in Fig. 3. It is a superposition of the probe and DUT spectra. If a modulation is not

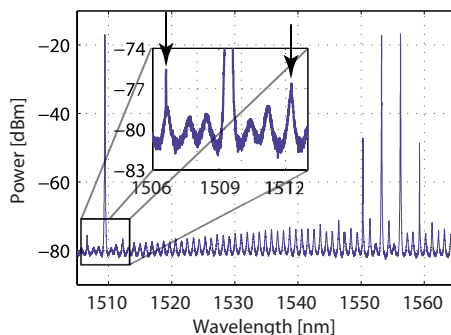


FIG. 3. (Color online) Optical spectrum of the first DUT under injection of the probe signal. In the inset, a zoom around the probe signal is shown, the arrows are placed to highlight the SBs around the probe.

present in the device, no side-band (SB) modulation would be observed. However, SBs are observed and localized at 1506.60 nm and 1512.26 nm. This happens even though there is no direct or external modulations applied to the DUT. Therefore, a modulation is generated resulting from the beating between the lasing modes. This is mostly visible in the upper side, i.e., in the lower wavelength range. The modulation frequency is directly determined by the probe's wavelength and one of its sideband wavelengths according to

$$\Delta f = c|1/\lambda_1 - 1/\lambda_2|, \quad (1)$$

where  $c$  is the speed of light and  $\lambda_{1,2}$  are the wavelengths of the probe signal and one of the SB, respectively. The error measured on the modulation frequency is given by

$$\text{err}(\Delta f) = c\Delta\lambda \sum_{i=1,2} 1/\lambda_i^2, \quad (2)$$

where  $\Delta\lambda$  is the OSA resolution. The frequency and the error measured for this DUT are  $372 \pm 5.27$  GHz, which corresponds to the separation between the two main modes of the DUT. It is worth mentioning that our method is limited by the resolution of our OSA. Its resolution is larger than that of the FT-IR but lower than that of the FROG method. For instance, the FT-IR interferometer has a 1.8 GHz resolution at 1550 nm while the FROG has a 200 fs temporal resolution, resulting in an error of 28 GHz in the spectral domain.

This terahertz measurement confirms the results achieved with the FROG method.<sup>1</sup> The beating produces a modulation of the material gain and the refractive index of the DUT active region, which modulates the amplitude and phase of these modes. A probe signal injected in the device experience these amplitude and phase modulations as well, with a decreasing efficiency as the probe wavelength is further away from the gain peak.

A second DUT, produced with the same layer composition, the same waveguide geometry and groove dimensions as that of the first DUT, has been designed to generate an electromagnetic wave at a frequency beyond 1 THz. Its length is 1.05 mm to avail of an enhancement in the FWM process. Its threshold current is measured at 26 mA. At a bias current of 81.15 mA, a voltage across the junction under 2 V and a temperature maintained at 25 °C, its optical spectrum features two main modes at 1554.8 nm and 1545.52 nm, separated by 1.1 THz, in good agreement with the groove pattern designed. The demonstration of terahertz generation is carried out using the experimental setup presented in Fig. 2 since it gives identical results to that of the FT-IR interferometer or the FROG method. The 1524.11 nm probe signal is set with a power of 5.5 dBm,  $\sim 20$  nm away from the main lasing modes. The DUT optical spectrum under probe optical injection is presented in Fig. 4. It consists of the DUT optical spectrum added to the probe spectrum. It presents a SB modulation particularly pronounced for the upper SB at 1515.20 nm. Using Eqs. (1) and (2), the modulation frequency is measured at  $1.157 \pm 0.005$  THz.

Terahertz signals generated by DUT1 and DUT2 have been measured by three different methods at a frequency of  $\sim 370$  GHz and by one method at  $\sim 1.15$  THz, respectively. For these devices, the gain dynamics supporting these terahertz modulations cannot be carrier-density pulsation but CH.<sup>7</sup> It is able to sustain this modulation frequency since the carrier-phonon scattering has a 650 fs typical characteristic time. In the inset of Fig. 1, the two main modes labeled 2 and

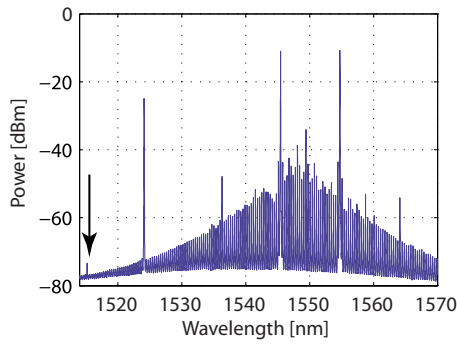


FIG. 4. (Color online) Optical spectrum of the second DUT under injection of the probe. The bias current is 81.15 mA and temperature is controlled at 25 °C. The arrow is placed to highlight the SB around the probe signal.

3 are surrounded by secondary modes, which present the effect of the modulation, in particular mode 1 on the left hand-side of the two main modes. The beatings between modes 1 and 2 and between modes 2 and 3 are at the same frequency, equal to 372 GHz FSR. The beatings produce a modulation of the carrier-gas temperature, consequently of the quasi-Fermi level and the gain and refractive index of the cavity, which affects the amplitude and the phase of each mode.<sup>8</sup> For instance, the beating between modes 1 and 2 is proportional to  $(E_1 E_2^*)$ , where \* stands for the conjugate signal and  $E_i$  for the electric field of the  $i$ th mode, expressed as  $E_{oi} \exp[j(\omega_i t + \varphi_i)]$  with  $E_{oi}$  being the amplitude of the electric field,  $\omega_i$  is its angular frequency, and  $\varphi_i$  is its phase noise. This beating introduces an amplitude and phase modulation of mode 2, which generates a SB modulation injected into mode 1, proportional to  $\chi^{(3)}(\omega_1, -\omega_2, \omega_1) E_2 (E_1 E_2^*)$  where  $\chi^{(3)}$  is the third order nonlinear susceptibility of the active layer. The SB phase is given by  $(\varphi_2 + \varphi_1 - \varphi_2 = \varphi_1)$  and corresponds to transfer of energy from mode 2 to mode 1, since the SB phase is  $\varphi_1$ . The beating between modes 2 and 3 is also at the same frequency. It is proportional to  $(E_2 E_3^*)$ , and it modulates mode 2 and produces a SB at mode 1 proportional to  $\chi^{(3)}(\omega_1, -\omega_3, \omega_2) E_2 (E_2 E_3^*)$  with a phase of  $(\varphi_2 + \varphi_2 - \varphi_3 = 2\varphi_2 - \varphi_3)$ . Thus, the phase of mode 1 is affected by the phase of modes 2 and 3 via this latter SB. This process is not limited to mode 1, it is repeated with all lasing modes. The phase noise of each is being correlated and reduced; consequently their optical linewidth is quenched. This reduction in the linewidth can be seen for mode 1 in the inset of Fig. 1. The correlation of the phase of each mode explains also why the 2 modes observed with the FROG method have a constant phase difference.<sup>1</sup>

With this type of device, there is an inherent passive mode-locking of the optical modes. The terahertz signal achieved benefits from this and the terahertz signal linewidth is narrower than the sum of the linewidth of the optical modes involved. The mechanism of passive mode-locking in lasers generating radio frequency (rf) waves has already been

demonstrated,<sup>9</sup> with an rf linewidth smaller than the sum of the lasing mode linewidths. It is originated by carrier density pulsation as the detuning between modes is  $< 100$  GHz.<sup>7</sup> The terahertz wave generation is based on similar FWM mechanism to that of rf, except it would involve CH as the detuning frequency is larger than 100 GHz. For even larger FSR on the order of 1.5 THz, the spectral hole burning would be the main FWM effect. Its characteristic time is 100 fs, which allows frequency detunings up to 10 THz. In this case, with this type of multimode lasers, dc-biased and at room temperature it would be possible to cover the entire terahertz spectrum.

It seems possible to generate a periodic modulation of the optical output of a multimode laser at a frequency equal to the FSR. The mode beating is supported by gain nonlinearities such as carrier density pulsation, CH, and spectral-hole-burning. In this paper we proposed a technique to determine and accurately measure a modulation from multimode semiconductor lasers. The achieved results have been compared with those from two other techniques showing excellent agreement. Using this method, we demonstrated that by controlling the FSR, a 1.15 THz emission is achievable with a grooved multimode laser biased at low current, under 100 mA, with a low voltage  $\sim 2$  V, and temperature controlled at 25 °C. This technique was based on the assumption that a modulation of the complex refractive index of the active layer is sustained by the carrier-phonon scattering. The modulation results from the beating of the lasing modes. The modulation frequency is set by the FSR selected by the groove pattern. The results by our technique corroborate this hypothesis. As the lasing modes are beating within the cavity, the FWM process benefits from an optimal overlap of the modes and an excellent mechanical stability. The carrier-heating mechanism results in a phase transfer of the lasing modes, hence passive mode-locking of the lasing modes.

The authors thank Science Foundation Ireland for its support under Project No. 05/RFP/0040 and the HEA PRTL14 INSPIRE.

<sup>1</sup>S. Latkowski, F. Surre, and P. Landais, *Appl. Phys. Lett.* **92**, 081109 (2008).

<sup>2</sup>P. Landais, Patent No. S2005/0251, Ireland (26 April 2005).

<sup>3</sup>K. J. Ebeling and L. A. Coldren, *J. Appl. Phys.* **54**, 2962 (1983).

<sup>4</sup>E. Bründermann, A. M. Linhart, H. P. Röser, O. D. Dubon, and W. L. Hansen, *Appl. Phys. Lett.* **68**, 1359 (1996).

<sup>5</sup>M. M. A. Belkin, F. Capasso, F. Xie, A. Belyanin, M. Fischer, A. Wittmann, and J. Faist, *Appl. Phys. Lett.* **92**, 201101 (2008).

<sup>6</sup>R. Nietzke, W. Elbässer, and A. N. Baranova, *Appl. Phys. Lett.* **58**, 554 (1991).

<sup>7</sup>G. Agrawal, *Appl. Phys. Lett.* **51**, 302 (1987).

<sup>8</sup>A. D'Ottavi, E. Iannone, A. Meccozzi, S. Scotti, P. Spano, R. Dall'Ara, G. Guekos, and J. Ecker, European Conference on Optical Communication (ECOC), 1994 (unpublished), p. 737.

<sup>9</sup>J. Renaudier, G. H. Duan, P. Landais, and P. Gallion, *IEEE J. Quantum Electron.* **43**, 147 (2007).